

PAPER • OPEN ACCESS

Distribution model of toxic agents and runoff phenomenon in flat aquatic regions

To cite this article: J G Vergaño-Salazar *et al* 2020 *J. Phys.: Conf. Ser.* **1514** 012004

View the [article online](#) for updates and enhancements.

You may also like

- [Characterization of hand movements using a low cost electromyography sensor](#)
G Laverde, S Salinas, D Montero et al.
- [Assessment of left ventricle dynamic from cardiac magnetic resonance imaging by means a correspondence approach](#)
A Bravo, M Vera and O Valbuena
- [Academic performance and mathematical processes under a causal model. Correlations found in three public institutions](#)
R Prada, R Fernández and C A Hernández



ECS
The
Electrochemical
Society
Advancing solid state &
electrochemical science & technology

DISCOVER
how sustainability
intersects with
electrochemistry & solid
state science research

Distribution model of toxic agents and runoff phenomenon in flat aquatic regions

J G Vergaño-Salazar¹, J F C A Meyer², F Córdova-Lepe¹, and E Duque Marín¹

¹ Facultad de Ciencias Básicas, Universidad Católica del Maule, Talca, Chile

² Departamento de Matemática Aplicada, Universidade Estadual de Campinas, Campinas, Brasil

E-mail: jgvs190@gmail.com, juan.vergano@alu.ucm.cl

Abstract. The study presents a model of distribution of toxic agents in flat aquatic regions such as lakes, lagoons, and coastal seas, two sources of pollution are modeled, one from the waste of industrial plants and another one, a product of the runoff phenomenon of the agricultural industry. Methodologically, a mathematical model based on the advection-diffusion equation is used, which allows knowing the concentration of the contaminant at all times in time for the given region. The problem system is described in its variational formulation in order to approximate its solution by the finite element method. The parameters used in the simulations are taken from secondary sources, in order to compare results and differences in the same scenarios included in other models.

1. Introduction

There are different and multiple sources of pollution for water resources, among the most important are: industrial plant waste, the expansion of cities and agriculture that emphasizes in production and uses fungicides and pesticides that are transported by the runoff phenomenon to the slopes of rivers and lagoons. Knowing the behavior of toxic agents that affect the aquatic regions is a first step towards the recovery and sustenance of water resources. This article aims to know the concentration and dynamics of toxic agents in a flat aquatic region, using the diffusion-advection equation to model two sources of pollution, one in the center of the region (point source of contamination) and another it is the source corresponding to the pollution due to the runoff phenomenon at the border.

2. Framework

Environmental pollution is one of the biggest global problems, with water being the most affected system [1–3], the pollution of water resources produced by industry is due to specific sources of pollution, in these wastes there is a greater amount of synthetic organic compounds and toxic metals such as: lead, mercury and cadmium [4,5]. On the other hand, urban expansion is a major producer of waste, since all toxic substances, such as sewage and rain, are frequently thrown into the water with oils and organic matter [3]. The modern agricultural industry that emphasizes production, uses fungicides and pesticides, which are transported by the runoff phenomenon, here runoff is the transport of existing toxic substances in the earth through the waters, especially



rainy waters and, to a small extent, to the waters that come from the irrigation of crops [2,3,5,6]. The toxicity potential of pollutants produced by agriculture is important, since they have a high toxic level of a non-biodegradable nature, such as: sodium, potassium, calcium, magnesium, some salts (nitrates, carbonates, phosphates, sulfates), acids and solid particles [2].

An example of this is the coverage of large areas of water by higher density substances such as oils and fats that reduce reoxygenation through the decrease in air-water interaction, that is, less oxygen and more absorbing solar radiation, which affect photosynthetic activity causing the death of the species that consume oxygen, another cause of the decrease in dissolved oxygen is mechanical contamination, which consists mainly of the deposit of mineral particles or organic [3,6].

3. Mathematical model

The phenomenon of diffusion is based on the conservation law [7,8] which states that: The rate of change of the concentration of particles per unit of time, is equal to the number of particles that enter the system minus the number of particles that leave more or less the rate of growth or degradation of the particles per unit of time [1]. Suppose that $\mathbf{V}(x, y)$ is the speed of the fluid, with a flow $\mathbf{J} = c\mathbf{V}$, where c represents the concentration of particles [4,5], from law Fick it is established that the flow is proportional to less the local gradient of the concentration, with this expression of the flow the equation is obtained: $\partial c / \partial t = \alpha \nabla^2 c \pm \sigma$ it is the diffusion equation [5,7,9]. It is denoted with α the diffusion coefficient of the toxic agent, then the term $\alpha \nabla^2 c$ it represents the diffusion of the contaminant. Because pollutants move in an aquatic environment, they experience an advective phenomenon, where v is the speed of the fluid, so the advection in the model is represented by the term $\nu \nabla c$, if σ is the degradation rate of the toxic, it has to σc represents the loss of pollutant in a unit of time, as mentioned earlier, there is a point source of contamination noted with $F(x, y, t) = F$. Thus Equation (1) that models the space-temporal concentration of a toxic agent in an aquatic environment is:

$$\frac{\partial c}{\partial t} - \alpha \nabla^2 c + \nu \nabla c + \sigma c = F, \quad (1)$$

where $c = c(x, y, t)$: toxic agent concentration, σ : constant pollutant degradation coefficient, α : diffusion coefficient of the toxic (considered constant), V : velocity field present in the fluid, F : describes the point source of contamination considered in the environment Ω during J . Equation (1) is called diffusion-advection equation, which can be rewritten as Equation (2).

$$\frac{\partial c}{\partial t} = \text{div}(\alpha \nabla c) - \text{div}(Vc) - \sigma c + F, \quad (2)$$

the initial condition is $c(x, y, 0) = c_0(x, y)$, $(x, y) \in \Omega$ and boundary conditions $\partial\Omega = \Gamma_0 \cup \Gamma_1$, where Γ_0 presents conditions at the edge of the homogeneous Von Neumann type and Γ_1 presents the non-homogeneous Dirichlet condition, that is, $\frac{\partial c}{\partial \eta} \Big|_{\Gamma_0} = 0$, with η the outer normal unit vector along the border Γ_0 de Ω and $c(x, y, t)|_{\Gamma_1} = g(x, y)$, which represents the contamination by the phenomenon of runoff from agricultural fields [10,11], then a model that describes the problem of contamination is defined as Equation (3):

$$\begin{cases} \frac{\partial c}{\partial t} = \text{div}(\alpha \nabla c) - \text{div}(Vc) + \sigma c + F, \\ c(x, y, 0) = c_0(x, y), \quad \forall (x, y) \in \Omega, \\ \frac{\partial c}{\partial \eta} \Big|_{\Gamma_0} = 0, \quad c(x, y, t)|_{\Gamma_1} = g(x, y) \forall t \in J. \end{cases} \quad (3)$$

4. Variational formulation

Problem for Equation (3) is presented in its classic or strong formulation, with the aim of approaching the solution, the formulation is used weak or variational using the derivative in the sense of distribution [12–15]. Internal products are defined in $L_2(\Omega)$ as Equation (4).

$$(f | g) = \int_{\Omega} f(x) g(x) ds. \quad \forall \quad (\nabla c | \nabla v) = \int_{\Omega} \left(\frac{\partial c}{\partial x} \frac{\partial v}{\partial x} + \frac{\partial c}{\partial y} \frac{\partial v}{\partial y} \right) ds. \quad (4)$$

Definition 1. Weak derived. Let β be a multi-index, $u, v \in L_{1,Loc}(\Omega)$ and $\int_{\Omega} u(x) \partial^{\beta} \eta(x) dx = (-1)^{|\beta|} \int_{\Omega} v(x) \eta(x) dx, \forall \eta \in C_0^{\infty}(\Omega)$. Then v is called the weak partial derivative of u in Ω and is denoted by $\partial^{\beta} u$.

In the space $H_0^1(\Omega) = \{u \in H^1(\Omega); u|_{\partial\Gamma_1} = 0\}$, the formulation in the sense of distributions of Equation (2) is Equation (5).

$$\int_{\Omega} \frac{\partial c}{\partial t} v ds = \int_{\Omega} \text{div}(\alpha \nabla c) v ds - \int_{\Omega} \text{div}(V c) v ds - \int_{\Omega} \sigma c v ds + \int_{\Omega} F v ds, \quad \forall v \in \mathcal{V} \quad (5)$$

Then, for the Green theorem, it has to Equation (6) is true as:

$$\int_{\Omega} \text{div}(\alpha \nabla v) v ds = - \int_{\Omega} \alpha \nabla c \cdot \nabla v ds + \alpha \int_{\partial\Omega} \frac{\partial c}{\partial \eta} v dr. \quad (6)$$

So, replacing Equation (6) in Equation (5) and considering internal products defined in $L_2(\Omega)$ and V it is a vector field independent of time and space, in addition to the homogeneous von Neumann type boundary condition $\frac{\partial c}{\partial \eta} \Big|_{\Gamma_0} = 0$, it has to $\int_{\partial\Omega} \frac{\partial c}{\partial \eta} v dr = 0, \forall v \in \mathcal{V}$, in this way the formulation in the sense of distribution of the problem is given by Equation (7).

$$\left(\frac{\partial c}{\partial t} | v \right) = -\alpha (\nabla c | \nabla v) - V (\nabla c | v) + \sigma c + F, \quad \forall v \in \mathcal{V}. \quad (7)$$

5. Approximation of solution

5.1. Galerkin method

To find a solution $c \in \mathcal{V}$ of the Equation (7), a solution is sought $c_h \in \mathcal{V}_h$ which is the closest to the solution $c \in \mathcal{V}$ [9, 16, 17], so that, the solution satisfies Equation (8) and Equation (9).

$$c_h = \sum_{j=1}^m c_j(t) \varphi_j(x, y) + \sum_{j=m+1}^n g_j(t) \varphi_j(x, y). \quad (8)$$

$$\frac{\partial c_h}{\partial t} = \sum_{j=1}^m \frac{\partial c_j}{\partial t} \varphi_j(x, y) + \sum_{j=m+1}^n \frac{\partial g_j(t)}{\partial t} \varphi_j(x, y), \quad \forall \varphi_j(x, y) = \varphi_i \in B. \quad (9)$$

Now replacing Equation (8) and Equation (9) in Equation (7) and using the $c_j(t) = c_j, v_j(t) = v_j$ notation, in addition, given the properties of the internal product and considering that V is a vector field independent of time and space, we have the system given by Equation (10).

$$\begin{aligned}
& \sum_{j=1}^m \frac{\partial c_j}{\partial t} (\varphi_j | \varphi_i) + \alpha \sum_{j=1}^m c_j (\nabla \varphi_j | \nabla \varphi_i) \\
& + V_1 \sum_{j=1}^m c_j \left(\frac{\partial \varphi_j}{\partial x} | \varphi_i \right) + V_2 \sum_{j=1}^m c_j \left(\frac{\partial \varphi_j}{\partial y} | \varphi_i \right) - \sum_{j=1}^m c_j (\sigma \varphi_j | \varphi_i) \\
& = - \sum_{j=m+1}^n \frac{\partial g_j}{\partial t} (\varphi_j | \varphi_i) - \alpha \sum_{j=m+1}^n g_j (\nabla \varphi_j | \nabla \varphi_i) - V_1 \sum_{j=m+1}^n g_j \left(\frac{\partial \varphi_j}{\partial x} | \varphi_i \right) \\
& - V_2 \sum_{j=m+1}^n g_j \left(\frac{\partial \varphi_j}{\partial y} | \varphi_i \right) - \sum_{j=m+1}^n g_j (\sigma \varphi_j | \varphi_i) + (F | \varphi_i) + \left(F | \sum_{j=1}^n v_j \varphi_j \right), \quad \forall \varphi_i \in B.
\end{aligned} \tag{10}$$

It show that Equation (10) corresponds to a linear system of ordinary differential equations in the variable t , with the initial condition that in its variational formulation is given by Equation (11).

$$(c_0(x, y) | \varphi_i) = \sum_{j=1}^m c_j(0) (\varphi_j | \varphi_i) + \sum_{j=m+1}^n c_j(0) (\varphi_j | \varphi_i), \quad \forall \varphi_i \in B. \tag{11}$$

5.2. Finite elements

Finite elements method allows spatial discretization in the domain of interest, by building a mesh to obtain a finite number of simple subdomains. To discretize the spatial variable, a rectangular domain Ω is taken. Since the selected elements are second order [12–15, 18, 19], a hexagonal base pyramid is constructed, as illustrated in the Figure (1).

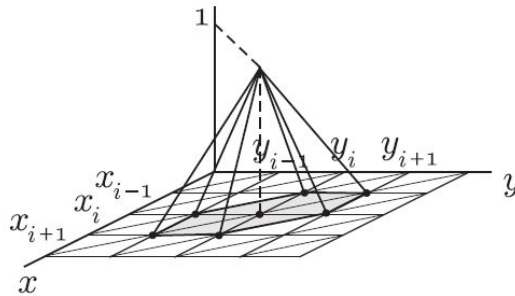


Figure 1. Pyramid for finite elements.

Figure (1) is the base of \mathcal{V}_h , whose elements are the test functions. The faces of the pyramid are the φ_i functions, for $i \in \{1, \dots, n\}$, which are defined in Equation (12).

$$\varphi_i = \begin{cases} \{x - x_{i-1}\} / \Delta x, & x = x_{i-1}; & y_i \leq y \leq y_{i+1} \\ \{y_{i+1} - y\} / \Delta y, & y = y_{i+1}, & x_{i-1} \leq x \leq x_i, \\ \{x_{i+1} \Delta y - x \Delta y + y_i \Delta x - y \Delta x\} / \{\Delta y \Delta x\}, & x_i \leq x \leq x_{i+1}, & y_i \leq y \leq y_{i+1}, \\ \{x_{i+1} - x\} / \Delta x, & x = x_{i+1}, & y_{i-1} \leq y \leq y_i, \\ \{y - y_{i-1}\} / \Delta y, & y = y_{i-1}, & x_i \leq x \leq x_{i+1}, \\ \{x \Delta y - x_i \Delta y + y \Delta x - y_{i-1} \Delta x\} / \{\Delta y \Delta x\}, & x_{i-1} \leq x \leq x_i, & y_{i-1} \leq y \leq y_i. \end{cases} \tag{12}$$

Making use of the functions defined by Equation (12), internal products are calculated for the triangles of the domain are given by Equation (13), Equation (14) and Equation (15) as.

$$(\varphi_j | \varphi_i) = \frac{\Delta x \Delta y}{24} \begin{bmatrix} 1 & \frac{1}{2} & \frac{1}{2} \\ \frac{1}{2} & 1 & \frac{1}{2} \\ \frac{1}{2} & \frac{1}{2} & 1 \end{bmatrix} \quad \text{and} \quad (\nabla \varphi_j | \nabla \varphi_i) = \frac{1}{2} \begin{bmatrix} \frac{\Delta y}{\Delta x} + \frac{\Delta x}{\Delta y} & -\frac{\Delta y}{\Delta x} & -\frac{\Delta x}{\Delta y} \\ -\frac{\Delta y}{\Delta x} & \frac{\Delta y}{\Delta x} & 0 \\ -\frac{\Delta x}{\Delta y} & 0 & \frac{\Delta x}{\Delta y} \end{bmatrix}. \quad (13)$$

For the odd triangle you have Equation (14).

$$\left(\frac{\partial \varphi_j}{\partial x} | \varphi_i \right) = \frac{\Delta y}{6} \begin{bmatrix} -1 & 1 & 0 \\ -1 & 1 & 0 \\ -1 & 1 & 0 \end{bmatrix} \quad \text{and} \quad \left(\frac{\partial \varphi_j}{\partial y} | \varphi_i \right) = \frac{\Delta x}{6} \begin{bmatrix} -1 & 0 & 1 \\ -1 & 0 & 1 \\ -1 & 0 & 1 \end{bmatrix}, \quad (14)$$

and for the even triangle we have Equation (15).

$$\left(\frac{\partial \varphi_j}{\partial x} | \varphi_i \right) = \frac{\Delta y}{6} \begin{bmatrix} 1 & -1 & 0 \\ 1 & -1 & 0 \\ 1 & -1 & 0 \end{bmatrix} \quad \text{and} \quad \left(\frac{\partial \varphi_j}{\partial y} | \varphi_i \right) = \frac{\Delta x}{6} \begin{bmatrix} 1 & 0 & -1 \\ 1 & 0 & -1 \\ 1 & 0 & -1 \end{bmatrix}. \quad (15)$$

Equation (13), Equation (14) and Equation (15) are called submatrices of stiffness.

5.3. Crank Nicolson method

Crank Nicolson method discretizes the temporal variable [11,20,21] of the Equation (10), to use this method, use is made of Equation (16).

$$\begin{aligned} c_j(t_n) &\simeq \frac{c_j^{(n+1)} + c_j^{(n)}}{2}, \quad g_j(t_n) \simeq \frac{g_j^{(n+1)} + g_j^{(n)}}{2} \\ \frac{\partial c_j(t_n)}{\partial t} &= \frac{c_j^{(n+1)} - c_j^{(n)}}{\Delta t}, \quad \frac{\partial g_j(t_n)}{\partial t} = \frac{g_j^{(n+1)} - g_j^{(n)}}{\Delta t}, \end{aligned} \quad (16)$$

$$\mathbf{A} \mathbf{p}^{(n+1)} = \mathbf{B} \mathbf{p}^{(n)} + \mathbf{D} \quad \text{and} \quad \mathbf{c}^0 = (\mathbf{c}_1^0, \mathbf{c}_2^0, \dots, \mathbf{c}_n^0).$$

Where the stiff \mathbf{A} , \mathbf{B} and \mathbf{D} matrices are shown in Equation (17).

$$\begin{aligned} a_{ij} &= (1 + \frac{\sigma \Delta t}{2}) (\varphi_j | \varphi_i) + \frac{\alpha \Delta t}{2} (\nabla \varphi_j | \nabla \varphi_i) + \frac{V_1 \Delta t}{2} \left(\frac{\partial \varphi_j}{\partial x} | \varphi_i \right) + \frac{V_2 \Delta t}{2} \left(\frac{\partial \varphi_j}{\partial y} | \varphi_i \right) \\ b_{ij} &= (1 - \frac{\sigma \Delta t}{2}) (\varphi_j | \varphi_i) - \frac{\alpha \Delta t}{2} (\nabla \varphi_j | \nabla \varphi_i) - \frac{V_1 \Delta t}{2} \left(\frac{\partial \varphi_j}{\partial x} | \varphi_i \right) - \frac{V_2 \Delta t}{2} \left(\frac{\partial \varphi_j}{\partial y} | \varphi_i \right) \\ d_{ij} &= - \left[\Delta t \frac{g_j^{(n+1)} + g_j^{(n)}}{2} (\varphi_j | \varphi_i) + \alpha \Delta t \frac{g_j^{(n+1)} + g_j^{(n)}}{2} (\nabla \varphi_j | \nabla \varphi_i) + V_1 \Delta t \frac{g_j^{(n+1)} + g_j^{(n)}}{2} \left(\frac{\partial \varphi_j}{\partial x} | \varphi_i \right) \right. \\ &\quad \left. + V_2 \Delta t \frac{g_j^{(n+1)} + g_j^{(n)}}{2} \left(\frac{\partial \varphi_j}{\partial y} | \varphi_i \right) + \Delta t \frac{g_j^{(n+1)} + g_j^{(n)}}{2} (\sigma \varphi_j | \varphi_i) \right] + \Delta t (F | \varphi_i). \end{aligned} \quad (17)$$

6. Numerical results and discussion

This work considers a flat aquatic region with two sources of pollution, one point in the bottom left and the other due to runoff as shown in Figure 2, Figure 3, Figure 4 and Figure 5. In [2,3,6] only interior sources of the domain are modeled and assume that there is no contamination at the border, which does not show the actual behavior of the concentration of pollutants, thus limiting the comparison of pollution flows, runoff contamination affects all places in the region as shown in Figure 4 and Figure 5, which is not evident in the results of [3,6]. As in [3,4,6,17] advective movement has a greater influence on the behavior of the contaminant, Figure 2 and Figure 3 show that changing the velocity field changes the dynamic behavior of the contamination. The parameters for these simulations were based in [6] where $\alpha = 0.5e^{-2}$, $\mu = 0.01$, $V_x = 0.001$ and $V_y = 0.13$, the convergence of the method is guaranteed by [22].

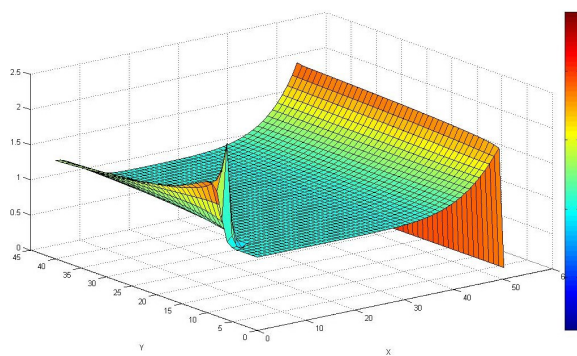


Figure 2. Pollutant in 50 days, V_x and V_y positive.

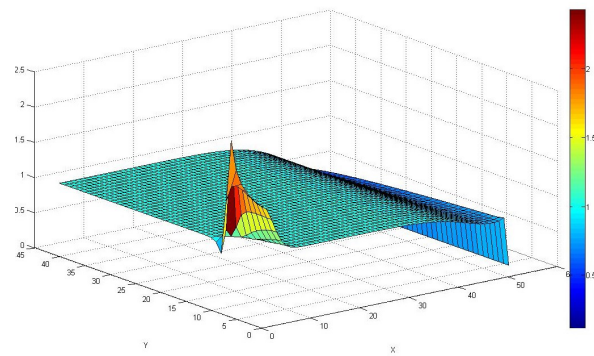


Figure 3. Pollutant in 50 days, V_x positive and V_y negative.

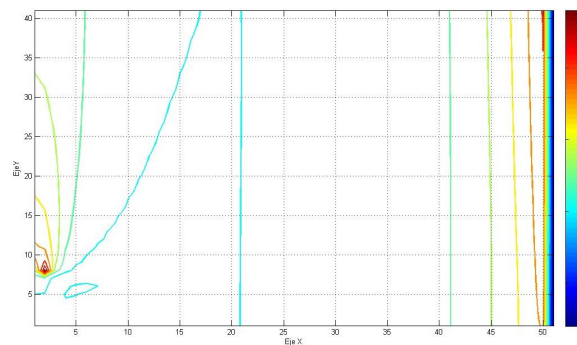


Figure 4. Contaminant contour in 50 days, V_x and V_y positive.

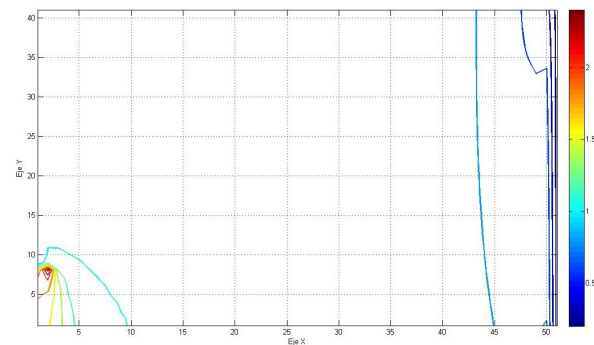


Figure 5. Contaminant contour in 50 days, V_x positive and V_y negative.

7. Conclusion

This study show that as the time increases, concentration of toxic at the point source is greater than the pollution due to runoff, having non-zero boundary conditions allows to know the real dynamics behavior of the toxic agents and do not limiting the comparison of contamination flows, the pollution value is higher in short times both at the point source within the region and at the border. The advective movement has a greater influence on the behavior of the pollutant which shows that the model reflects the physical characteristics of the environment, the concentration of pollutant is sensitive to the direction they can take winds, that is, the movement of pollutants depends largely on the velocity field.

References

- [1] Cantrell R & Cosner C 1996 Practical persistence in ecological models via comparison methods *Proceedings of Royal Society in Edinburgh* **126**(2) 247
- [2] Diniz G 2003 *Dispersão de poluentes num sistema ar-água: modelagem, aproximação e aplicações* (Campinas: Universidade Estadual de Campinas)
- [3] Oliveira F 2003 *O comportamento evolutivo de uma mancha de óleo na Bahia de Ilha Grande, RJ: modelagem, análise numérica e simulações* (Campinas: Universidade Estadual de Campinas)
- [4] Brinkman H 1947 A calculation of the viscous force exerted by a flowing fluid on a dense swarm of particles *Applied Scientific Research* **A1** 27
- [5] Brinkman H 1947 On the permeability of media consisting of closely packed porous particles *Applied Scientific Research* **A1** 81
- [6] Sossae R 2003 *A presença evolutiva de um material impactante e seu efeito no transiente populacional de espécies interativas: modelagem e simulação* (Campinas: Universidade Estadual de Campinas)
- [7] Alonso A and Valli A 1999 An optimal domain decomposition preconditioner for low-frequency time harmonic Maxwell equations *Math. Comp.* **68** 607
- [8] Anaya V, Mora D, Reales C & Ruiz-Baier R 2015 Stabilidad mixed approximation of axisymmetric Brinkman flows *ESAIM Math. Model. Numer. Anal.* **49** 855
- [9] Davis T A 2004 Algorithm 832: UMFPACK V4.3—An unsymmetric-pattern multifrontal method *ACM Transactions on Mathematical Software* **30** 196
- [10] Bertoluzza S, Chabannes V, Prud'Homme C & Szopos M 2017 Boundary conditions involving pressure for the Stokes problem and applications in computational hemodynamics *Comput. Methods. Appl. Mech. Engrg.* **322** 58
- [11] Burman E & Hansbo P 2006 Edge stabilization for the generalized Stokes problem: A continuous interior penalty method *Comput. Meth. Appl. Mech. Engrg.* **195** 2393
- [12] Amoura K, Azaiez M, Bernardi C, Chorfi N & Saadi S 2011 Finite-element analysis of a static fluid-solid interaction problem *IMA Journal of Numerical Analysis* **31** 886
- [13] Bustinza R, Gatica G N and González M 2005 A mixed finite element method for the generalized Stokes problem *Int. J. Numer. Meth. Fluids.* **49** 877
- [14] Girault A & Raviart A 1980 *Finite Element Methods for Navier-Stokes Equations, Theory and Algorithms* (Berlin: Springer-Verlag)
- [15] Monk P 2003 *Finite Element Methods for Maxwell's Equations* (Oxford: Clarendon Press)
- [16] Barrios T P, Bustinza R, García G C, Hernández E 2012 On stabilized mixed methods for generalized Stokes problem based on the velocity-pseudostress formulation: A priori error estimates *Comput. Methods Appl. Mech. Engrg.* **237-240** 78
- [17] Anaya V, Mora D, Ruiz-Baier R 2017 Pure vorticity formulation and Galerkin discretization for the Brinkman equations *IMA Journal of Numerical Analysis* **37**(4) 2020
- [18] Bramble J H and Hilbert S R 1970 Estimation of linear functionals on Sobolev spaces with application to Fourier transforms and spline interpolation *SIAM J. Numer. Anal.* **7**(1) 112
- [19] Gusman J, Neilan M 2012 A family of nonconforming elements for the Brinkman problem *IMA J. Numer. Anal.* **32**(4) 1484
- [20] Amoura K, Azaiez M, Bernardi C, Chorfi N, Saadi S 2007 Spectral element discretization of the vorticity, velocity and pressure formulation of the Navier-Stokes problem *Calcolo* **44**(3) 165
- [21] Bernardi C and Chorfi N 2007 Spectral discretization of the vorticity, velocity, and pressure formulation of the Stokes problem *SIAM J. Numer. Anal.* **44**(2) 826
- [22] Karlsen K H, Karper T K 2012 A convergent mixed method for the Stokes approximation of viscous compressible flow *IMA J. Numer. Anal.* **32**(3) 725